

Distribution-aware Block-sparse Recovery via Convex Optimization

Sajad Daei, Farzan Haddadi, Arash Amini

Abstract—We study the problem of reconstructing a block-sparse signal from compressively sampled measurements. In certain applications, in addition to the inherent block-sparse structure of the signal, some prior information about the block support, i.e. blocks containing non-zero elements, might be available. Although many block-sparse recovery algorithms have been investigated in Bayesian framework, it is still unclear how to incorporate the information about the probability of occurrence into regularization-based block-sparse recovery in an optimal sense. In this work, we bridge between these fields by the aid of a new concept in conic integral geometry. Specifically, we solve a weighted optimization problem when the prior distribution about the block support is available. Moreover, we obtain the unique weights that minimize the expected required number of measurements. Our simulations on both synthetic and real data confirm that these weights considerably decrease the required sample complexity.

Index Terms—Block sparse recovery, Bayesian information, Conic integral geometry, Convex optimization.

I. INTRODUCTION

COMPRESSED Sensing (CS) has emerged in the past decade as a modern technique for recovering a sparse vector $\mathbf{x} \in \mathbb{R}^n$ from compressed measurements (see [1], [2] for more explanations about this field). In this work, we consider signals $\mathbf{x} \in \mathbb{R}^n$ that have a block-sparse structure, namely their non-zero entries appear in blocks. This property has been referred in the literature as block sparsity. It is common to use the following optimization problem for recovering the signal \mathbf{x} from compressive measurements.

$$\begin{aligned} P_{1,2}^\eta : \quad & \min_{\mathbf{z} \in \mathbb{R}^n} \|\mathbf{z}\|_{1,2} := \sum_{b=1}^q \|\mathbf{z}_{\mathcal{V}_b}\|_2 \\ & \|\mathbf{A}\mathbf{z} - \mathbf{y}\|_2 \leq \eta, \end{aligned} \quad (1)$$

where $\mathbf{A} \in \mathbb{R}^{m \times n}$ represents a fat measurement matrix with $m \ll n$, $\{\mathcal{V}_b\}_{b=1}^q$ are the default disjoint blocks of size $\{k_b\}_{b=1}^q$ that partition the set $\{1, \dots, n\}$, $\mathbf{y} := \mathbf{A}\mathbf{x} + \mathbf{e} \in \mathbb{R}^m$ is the observation vector¹, \mathbf{e} is the noise term which is considered to be i.i.d. Gaussian with variance σ^2 , and η is an upper-bound for $\|\mathbf{e}\|_2$. Most of the earlier literature in block-sparse recovery is focused on the case of single constraint $\|\mathbf{A}\mathbf{z} - \mathbf{y}\|_2 \leq \eta$. However, in many applications such as DNA micro-arrays [3], [4], computational neuroscience [5] multi-band signal reconstruction, multiple measurement vector (MMV) problem

[6], and the reconstruction of signals in union of subspaces [7], [8] [9], [10], there exist additional information (or alternatively additional constraints in $P_{1,2}^\eta$) about the signal of interest. In this work, we explore the benefits of having access to extra information about the distribution of the block support (blocks containing non-zero elements) on the required number of measurements. To this end, we propose the optimization problem

$$\begin{aligned} P_{1,2,w}^\eta : \quad & \min_{\mathbf{z} \in \mathbb{R}^n} \|\mathbf{z}\|_{1,2,w} := \sum_{b=1}^q w_b \|\mathbf{z}_{\mathcal{V}_b}\|_2 \\ & \|\mathbf{y} - \mathbf{A}\mathbf{z}\|_2 \leq \eta, \\ & \mathbf{z} \in \mathcal{M} \end{aligned}$$

where the quantities $w_b, b = 1, \dots, q$ are some positive scalars, $\mathbf{w} := [w_1, \dots, w_q]^T$ and \mathcal{M} is some predefined model that restricts the feasible set of the solution. Specifically, we consider two new models for prior information that are of practical interest:

- **Model 1 (Prior distribution)** : We assume that the prior distribution of the block support is available. Under this setting, there are known probabilities associated with each block index $b \in \{1, \dots, q\}$. Namely,

$$\mathbb{P}(b \in \text{bsupp}(\mathbf{x})) = p_b \quad b = 1, \dots, q, \quad (2)$$

where $\text{bsupp}(\cdot)$ returns the block support of a vector.

- **Model 2 (Multiple Bayesian estimates)**: We consider L independent Bayesian estimates of $\text{bsupp}(\mathbf{x})$ i.e. $\{\mathcal{P}_i\}_{i=1}^L$ with accuracies

$$\alpha_i = \mathbb{P}(\mathcal{P}_i \subset \text{bsupp}(\mathbf{x})) \quad i = 1, \dots, L. \quad (3)$$

We assume, without loss of generality, α_i 's sum to unity. To each subset $\mathcal{P}_i \subset \{1, \dots, q\}$, we assign a fixed weight ω_i . In fact, it holds that

$$\mathbf{w} = \sum_{i=1}^L \omega_i \mathbf{1}_{\mathcal{P}_i} \in \mathbb{R}^q, \quad (4)$$

where $\mathbf{1}_C$ is the indicator function of the set C .

In this work, we obtain the weights $\mathbf{w}^* \in \mathbb{R}^q$ and $\boldsymbol{\omega}^* \in \mathbb{R}^L$ that minimize a threshold m_0 describing the expected number of required measurements for Models 1 and 2, respectively. Our approach is to find a suitable upper-bound for m_0 . The bound is not necessarily tight but leads to closed-form expressions for $\mathbf{w} \in \mathbb{R}^q$ and $\boldsymbol{\omega} \in \mathbb{R}^L$ in Models 1 and 2, respectively. Availability of the parameters (p_b 's and α_i 's) associated with Models 1 and 2 is feasible in certain practical scenarios. For instance, they might be obtained from previous

S. Daei and F. Haddadi are with the School of Electrical Engineering, Iran University of Science & Technology. A. Amini is with EE department, Sharif University of Technology.

¹Our analysis holds for both real and complex-valued signals and measurements.

signal estimation in a dynamic scenario or from the statistic of previous training data. We further show that how Model 1 and 2 apply to brain functional magnetic resonance imaging (fMRI) reconstruction and direction of arrival (DOA) estimation, respectively (see sections I-B,III). It often occurs in practice that the parameters p_b 's and α_i 's are not accurately accessible, but only an approximation is available. Our last contribution in this work is about this challenge. In fact, we show that our method of obtaining the optimal weights w^* and ω^* is robust to small changes of p_b and α_i as long as $p_b \gtrsim \frac{1}{10}$ and $\alpha_i \gtrsim \frac{1}{10}$. It is worth mentioning that in this work, two structures are used to construct the measurement matrix $\mathbf{A}_{m \times n}$: randomly subsampled discrete Fourier transform (DFT)² and i.i.d. standard normal distribution. The former lies in the structure of DOA estimation (see subsection I-B) while we use the latter for fMRI reconstruction. Although, at first look, might be different, these two distributions have a common property making them usable in our conic geometry approach [11, Theorem 1]; in fact, for both, null space of $\mathbf{A}_{m \times n}$ is drawn uniformly at random from Grassmann manifold of subspaces of dimension $n - m$.

A. Related works and Key Differences

CS in presence of prior information has been studied in different signal models. While a large part of research (see for example [12]–[17]) deals with deterministic signal models, only a few works (see [18]–[20]) have investigated random signal models with Bayesian information. In the deterministic model, the ground truth signal has intersected with a few sets which called support estimates. The contributing level of each set to the support is available to the experimenter [12], [13]. This exact situation is investigated in [17]. They propose a non-uniform model for capturing deterministic prior information. The work [19] considers a probabilistic model where there is a continuous shape function describing the probability of contributing each element to the support. The authors obtain an upper-bound for failure probability of weighted ℓ_1 minimization. Their approach is based on calculating the internal and external angles of a weighted cross polytope. With a different approach, [20] has investigated a discrete measure for Bayesian information (a special case of Model 1 with $k = 1$). They relate the weights of weighted ℓ_1 minimization to the discrete probability distribution by minimizing the expected intrinsic volumes of a weighted cone.

In some certain applications, the signal of interest is block or joint sparse³ and knowing the exact element-wise distribution might be infeasible. Rather, an approximate block distribution (Model 1 of our work) is available to the experimenter. From prior arts, it seems unclear how to make use of such information in an optimal sense. Moreover, in Model 2 of our work, we consider multiple probabilistic support or block support estimators; the case that has not been studied so far for sparse or block-sparse regimes.

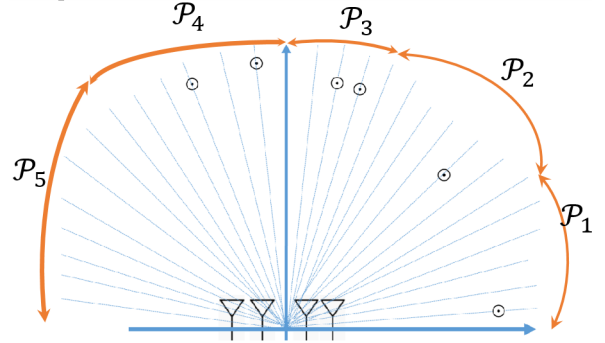


Fig. 1. Schematic diagram of DOA estimation of far-field sources. The angular half-space is divided into $q = 30$ angular clusters $\{\mathcal{V}_b\}_{b=1}^q$ with equal length. The associated parameters corresponding to Model 2 are $L = 5$, $\alpha_1 = \frac{1}{6}$, $\alpha_2 = \frac{1}{6}$, $\alpha_3 = \frac{1}{2}$, $\alpha_4 = \frac{1}{3}$ and $\alpha_5 = 0$.

B. Broadband DOA Estimation

Suppose that s far-field broadband signals $\{x_i(t, f)\}_{i=1}^s$ in the frequency range $f \in [f_L, f_H]$ incident on an q -element uniform linear array (ULA). The received signal in m sensors at time t and l -th frequency bin can be expressed as:

$$\mathbf{y}(t, f_l) = \sum_{i=1}^s \mathbf{a}_i(f_l) x_i(t, f_l) + \mathbf{e}(t, f_l) \in \mathbb{C}^m, \quad (5)$$

where $\mathbf{a}_i(f_l) := [1, \dots, e^{-j2\pi f_l \frac{(q-1)d}{c} \sin(\theta_i)}]^T$ is the steering vector, c is the propagation velocity, d is the inter-sensor spacing and $\mathbf{e}(t, f_l)$ is a Gaussian noise term with variance σ^2 . In practice, one has to take several snapshots $\{\mathbf{y}(t, f_l)\}_{t=1}^k$. This temporal redundancy is crucial in practice since the array size is limited due to physical constraints [21], [22]. Consequently, one may write

$$\begin{aligned} \mathbf{Y}(f_l) &:= [\mathbf{y}(1, f_l), \dots, \mathbf{y}(k, f_l)] = \\ \mathbf{A}(f_l) \mathbf{X}(f_l) + \mathbf{E}(f_l) &\in \mathbb{C}^{m \times k}, \end{aligned} \quad (6)$$

where $\mathbf{X}(f_l) = [\mathbf{x}(1, f_l), \dots, \mathbf{x}(q, f_l)] \in \mathbb{C}^{q \times k}$, $\mathbf{A}(f_l) = [\mathbf{a}_1(f_l), \dots, \mathbf{a}_q(f_l)] \in \mathbb{C}^{m \times q}$ and $\mathbf{E}(f_l) \in \mathbb{C}^{m \times k}$ is defined similarly. If the sources is time-invariant over the period of snapshotting, then for all $t = 1, \dots, k$ the non-zero dominant peaks in $\mathbf{x}(t, f_l)$ occur at the same locations corresponding to the ground truth DOAs. Hence, DOA estimation can be cast as recovering a joint sparse signal $\mathbf{X}(f_l)$ from $\mathbf{Y}(f_l)$. In addition, it is realistic for a radar engineer to know the probability of appearing the ground truth DOAs in some angular bands [23] (see Figure 1 for a schematic model of this scenario).

Notation. Throughout, scalars are denoted by lowercase letters, vectors by lowercase boldface letters, and matrices by uppercase boldface letters. The i th element of a vector \mathbf{x} is shown either by $x(i)$ or x_i . \mathcal{C}° denotes the polar of a cone \mathcal{C} . We show sets (e.g. \mathcal{B}) by calligraphic uppercase letters. $\bar{\mathcal{B}}$ is used to represent the complement $\{1, \dots, n\} \setminus \mathcal{B}$ of a set $\mathcal{B} \subset \{1, \dots, n\}$. $\mathbf{g} \in \mathbb{R}^n$ is a vector with standard normal distribution. The performance of an image $\widehat{\mathbf{X}} \in \mathbb{R}^{n_1 \times n_2}$ is measured by peak signal to noise ratio (PSNR) given by:

$$\text{PSNR}(\mathbf{X}, \widehat{\mathbf{X}}) = 20 \log_{10} \left(\frac{\|\mathbf{X}\|_{\infty} \sqrt{n_1 n_2}}{\|\mathbf{X} - \widehat{\mathbf{X}}\|_F} \right), \quad (7)$$

²Only a random subset of the rows of DFT matrix is observed.

³In this case, the non-zero blocks have common support.

where \mathbf{X} is the true image and $\|\cdot\|_\infty$ returns the maximum intensity.

II. MAIN RESULTS

Before stating our main results, we introduce two concepts from conic integral geometry that are used in our analysis.

Descent cone: Let \mathbf{x} be a vector and f be its structure inducing convex function. Then, the set of decent directions forms a convex set defined by:

$$\mathcal{D}(f, \mathbf{x}) = \bigcup_{t \geq 0} \{z \in \mathbb{C}^n : f(\mathbf{x} + tz) \leq f(\mathbf{x})\}. \quad (8)$$

Statistical dimension: It is shown in [11] that statistical dimension of the above decent cone defined by

$$\delta(\mathcal{D}(f, \mathbf{x})) := \mathbb{E} \text{dist}^2(\mathbf{g}, \mathcal{D}(f, \mathbf{x})^\circ), \quad (9)$$

specifies the required number of measurements (i.e. m) that

$$P_f : \min_{z \in \mathbb{C}^n} f(z) \quad \text{s.t.} \quad \mathbf{y}_{m \times 1} = \mathbf{A}z \quad (10)$$

needs for perfect recovery. Define the expected number of measurements needed for $P_{1,2,w}$ as

$$\bar{m} := \mathbb{E}_{\mathbf{x}} \delta(\mathcal{D}(\|\cdot\|_{1,2,w}, \mathbf{x})). \quad (11)$$

Then, we call the weights that minimize \bar{m} optimal in sense of expected sample complexity. In the following propositions, we obtain closed-form solutions for optimal weights in case that \mathbf{x} satisfies Model 1 and 2. The proofs are provided in Appendix A.

Proposition 1. *Let $\mathbf{x} \in \mathbb{C}^n$ satisfies Model 1 with parameter $\mathbf{p} = [p_1, \dots, p_q]^T$. Then, the optimal weights $\mathbf{w}^* = [w_1^*, \dots, w_q^*]^T$ in $P_{1,2,w}$ are obtained by solving the following equations simultaneously:*

$$\frac{p_b}{1-p_b} w_b^* = \frac{1}{2^{\frac{k_b}{2}-1} \Gamma(\frac{k_b}{2})} \int_{w_b^*}^{\infty} (u - w_b^*) u^{k_b-1} e^{-\frac{u^2}{2}} du \quad (12)$$

$$b = 1, \dots, q.$$

Proposition 2. *Let $\mathbf{x} \in \mathbb{C}^n$ be decomposed into q blocks \mathcal{V}_b of equal size k . Assume that there exist L independent Bayesian estimates $\{\mathcal{P}_i\}_{i=1}^L$ of $\text{bsupp}(\mathbf{x})$ with parameter $\boldsymbol{\alpha} = [\alpha_1, \dots, \alpha_L]^T$. Then, the optimal weights $\boldsymbol{\omega}^* = [\omega_1^*, \dots, \omega_L^*]^T$ in Model 2 are obtained by*

$$\frac{\alpha_i}{1-\alpha_i} \omega_i^* = \frac{1}{2^{\frac{k}{2}-1} \Gamma(\frac{k}{2})} \int_{\omega_i^*}^{\infty} (u - \omega_i^*) u^{k-1} e^{-\frac{u^2}{2}} du \quad (13)$$

$$i = 1, \dots, L.$$

In applications, it is of important practical value to know how the inaccuracies of p_b and α_i in Model 1 and 2, respectively, affect the optimal weights. The following theorem is about this challenge.

Theorem 1. *Assume that \mathbf{p} and \mathbf{p}' be the true and approximate estimate of $\text{bsupp}(\mathbf{x})$, respectively. Let \mathbf{w} and \mathbf{w}' be the*

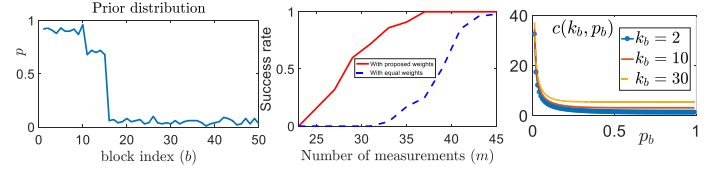


Fig. 2. The middle image compares the success rate of $P_{1,2,w^*}^0$ with that in $P_{1,2}^0$ when there exists a prior distribution $\mathbf{p} \in \mathbb{R}^q$ (depicted in the left image) about the block indexes $\{1, \dots, 50\}$. The optimal weight \mathbf{w}^* is obtained by (12). The right image represents $c(k_b, p_b)$ in Theorem 11 for different k_b 's.

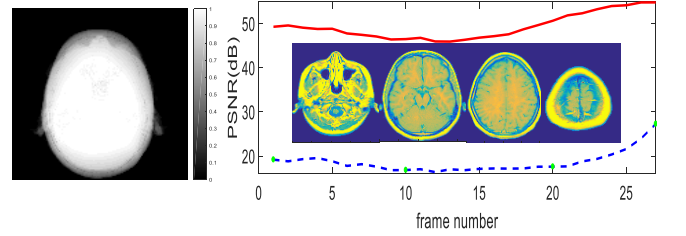


Fig. 3. Recovery of frames 1 to 27 of a fMRI video scan. The measurement matrix has i.i.d. Gaussian entries and $m = 9830$ measurements are taken. In the right image, recovery with $P_{1,2}^\eta$ is shown in the dashed line while recovery using $P_{1,2,w^*}^\eta$ is shown in the solid line. The prior distribution $\mathbf{p} \in \mathbb{R}^q$ that is used to calculate \mathbf{w}^* via (12) is depicted in the left image. The used parameters are $k_b = 1$ for all b and $q = 128^2 = 16384$. Selected true frames are also displayed in the right image, with green markers showing where these frames correspond to the PSNR of $P_{1,2}^\eta$.

optimal weights corresponding to \mathbf{p} , and \mathbf{p}' . Then, there exists a constant $c(k_b, p_b)$ such that

$$|w_b - w'_b| \leq c(k_b, p_b) |p_b - p'_b| \quad b = 1, \dots, q$$

$$c(k_b, p_b) := \frac{\left(\sqrt{2} h(p_b) \left(\Gamma\left(\frac{k_b}{2}\right) - \gamma\left(\frac{k_b}{2}, \frac{h(p_b)^2}{2}\right) \right) + 2\gamma\left(\frac{k_b}{2}, \frac{h(p_b)^2}{2}\right) \right)^2}{2\sqrt{2} \Gamma\left(\frac{k_b}{2}\right) \gamma\left(\frac{k_b}{2}, \frac{h(p_b)^2}{2}\right)} \quad (14)$$

where $\gamma(a, z) := \int_z^\infty u^{a-1} e^{-u} du$ is incomplete gamma function and $h(\cdot) : p_b \rightarrow w_b$ is the nonlinear function in (12).

From the above theorem and the right image of Figure 2, one can infer that the method of obtaining w_b^* and ω_i^* is robust to slight changes of p_b and α_i as long as $p_b \gtrsim \frac{1}{10}$ and $\alpha_i \gtrsim \frac{1}{10}$.

III. SIMULATIONS

In the first experiment, we construct a random block-sparse $\mathbf{x} \in \mathbb{R}^{250}$, whose building blocks \mathcal{V}_b have equal size $k = 5$. The probability of activating each block is taken from the vector \mathbf{p} depicted in the left image of Figure 2. Then, this signal is observed through a measurement matrix $\mathbf{A} \in \mathbb{R}^{m \times 250}$, of which the elements are drawn from i.i.d. standard normal distribution. We obtain the optimal weights \mathbf{w}^* corresponding to \mathbf{p} by solving (12). In the middle image of Figure 2, we plot the success rate as a function of m . For each m , we average over 100 realizations of \mathbf{A} and \mathbf{x} . As turns out, $P_{1,2,w^*}$ needs less measurements than $P_{1,2}$.

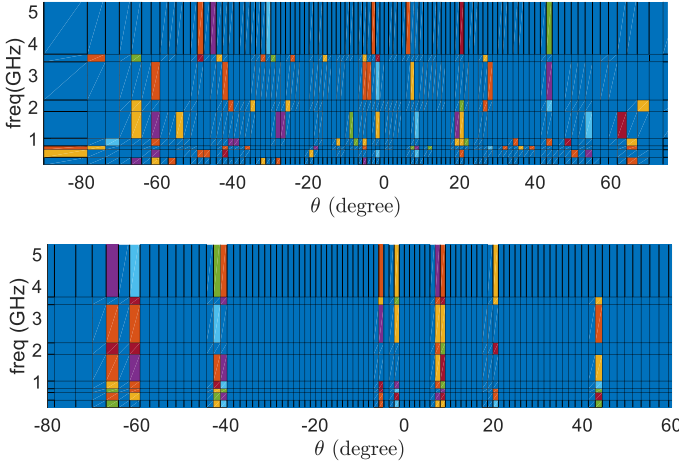


Fig. 4. Broadband DOA estimation for 10 sources using an $m = 15$ sensor ULA. The associated parameters are $k = 10$, $q = 100$, $d = 5$, $c = 3 \times 10^8$, and $\sigma = 1$. The accuracies corresponding to three Bayesian estimates are $\alpha_1 = \frac{4}{5}$, $\alpha_2 = \frac{2}{3}$, and $\alpha_3 = 0$. The top and bottom images correspond to the recovery using $P_{1,2}^\eta$ and $P_{1,2,\mathcal{D}\omega^*}^\eta$, respectively, where $\mathcal{D} := [1\mathcal{P}_1, 1\mathcal{P}_2, 1\mathcal{P}_3]$ and ω^* is calculated using (13).

In the second experiment, we test brain fMRI reconstruction of $n_1 \times n_2$ images when there exists a two dimensional prior distribution (the left image in Figure 3). We utilize 27 frames of a MRI video scan, each of which contains 128×128 pixels ($k_b = 1 \forall b$ and $q = 128^2 = 16384$), and consider only the gray scale components. The measurement matrix $\mathbf{A} \in \mathbb{R}^{9830 \times 16384}$ for each frame is chosen from an i.i.d. standard normal distribution. Also, the additive noise e is chosen to be i.i.d. Gaussian with variance $\frac{1}{100}$. We implement two recovery programs $P_{1,2}^\eta$ and $P_{1,2,\omega^*}^\eta$ (ω^* is obtained by (12)) using TFOCS package [24]. From the right image of Figure 3, one can see that, for a fixed $m = 9830$ and with our optimal weighting strategy, $P_{1,2,\omega^*}^\eta$ clearly acts better than $P_{1,2}^\eta$ (leading to PSNR values about 30dB higher than that in $P_{1,2}^\eta$).

In the last experiment, we test DOA estimation using broadband signals (see Subsection I-B and Figure 1). The angular half-space $[-90^\circ, 90^\circ]$ is divided into $q = 100$ angular clusters (grids). For each frequency bin $f_l \in [0, 5]$ GHz, we take $k = 10$ snapshots. We assume that there exist three ($L = 3$) Bayesian estimates \mathcal{P}_i with accuracies $\alpha_1 = \frac{4}{5}$, $\alpha_2 = \frac{2}{3}$, and $\alpha_3 = 0$. Also, we use $m = 15$ sensors for recovering $s = 10$ ground truth sources and implement the optimization problems $P_{1,2}^\eta$ and $P_{1,2,\omega^*}^\eta$ where $\omega^* = \sum_{i=1}^L \omega_i^* \mathbf{1}_{\mathcal{P}_i}$. ω_i^* 's are obtained using (13). As turns out from Figure 4, while $P_{1,2}^\eta$ detects many nonexisting sources with spurious DOAs, $P_{1,2,\omega^*}^\eta$ locates the ground truth sources correctly. This in turn suggests that our optimal weighting strategy considerably decreases the required number of sensors.

APPENDIX

A. Proof of Propositions 1 and 2

Proof. Since $\delta(\mathcal{D}(\|\cdot\|_{1,2,\mathbf{w}}, \mathbf{x}))$ only depends on $\text{bsupp}(\mathbf{x})$ and \mathbf{w} , we show it by $\delta(\mathcal{D}(\mathcal{B}, \mathbf{w}))$. It holds that:

$$\bar{m} = \mathbb{E}_{\mathbf{x}} \delta(\mathcal{D}(\text{bsupp}(\mathbf{x}), \mathbf{w})) =$$

$$\sum_{\mathcal{B} \subset [q]} \delta(\mathcal{D}(\mathcal{B}, \mathbf{w})) \mathbb{P}_{\mathbf{x}} \{\text{bsupp}(\mathbf{x}) = \mathcal{B}\} := \sum_{\mathcal{B} \subset [q]} \delta(\mathcal{D}(\mathcal{B}, \mathbf{w})) q_{\mathcal{B}} \quad (15)$$

We proceed by using an upper-bound for $\delta(\mathcal{D}(\mathcal{B}, \mathbf{w}))$ a special case of which is obtained in [17, Lemma 1].

Lemma 1. *The statistical dimension of descent cone of any vector $\mathbf{x}_{n \times 1}$ with $\text{bsupp}(\mathbf{x}) = \mathcal{B}$ satisfies:*

$$\delta(\mathcal{D}(\|\cdot\|_{1,2,\mathbf{w}}, \mathbf{x})) = \delta(\mathcal{D}(\mathcal{B}, \mathbf{w})) \leq \inf_{t \geq 0} \left(\sum_{b \in \mathcal{B}} (k_b + (tw_b)^2) + \frac{1}{2^{\frac{k_b}{2}-1} \Gamma(\frac{k_b}{2})} \sum_{b \in \bar{\mathcal{B}}} \phi_B(tw_b, k_b) \right),$$

$$\text{with } \phi_B(z, k) := \int_z^\infty (u-z)^2 u^{k-1} \exp(-\frac{u^2}{2}) du.$$

Moreover, the minimum achieved at a unique $t \geq 0$. The inequality is in fact equality in the asymptotic case ($q \rightarrow \infty$) [17, Proposition 3].

Thus, by the aid of Lemma 1, it holds that

$$\begin{aligned} \bar{m} &= \sum_{\mathcal{B} \subset [q]} q_{\mathcal{B}} \inf_{t \geq 0} \left(\sum_{b \in \mathcal{B}} (k_b + (tw_b)^2) + \frac{1}{2^{\frac{k_b}{2}-1} \Gamma(\frac{k_b}{2})} \sum_{b \in \bar{\mathcal{B}}} \phi_B(tw_b, k_b) \right) \\ &\leq \inf_{t \geq 0} \left(\sum_{\mathcal{B} \subset [q]} q_{\mathcal{B}} \left(\sum_{b \in \mathcal{B}} (k_b + (tw_b)^2) + \frac{1}{2^{\frac{k_b}{2}-1} \Gamma(\frac{k_b}{2})} \sum_{b \in \bar{\mathcal{B}}} \phi_B(tw_b, k_b) \right) \right) \\ &= \inf_{t \geq 0} \sum_{b=1}^q (k_b + t^2 w_b^2) \left(\sum_{\mathcal{B} \ni b} q_{\mathcal{B}} \right) + \left(\sum_{\mathcal{B} \not\ni b} q_{\mathcal{B}} \right) \frac{1}{2^{\frac{k_b}{2}-1} \Gamma(\frac{k_b}{2})} \phi_B(tw_b, k_b) \end{aligned}$$

By using $p_b := \mathbb{P}(b \in \text{bsupp}(\mathbf{x})) = \sum_{\mathcal{B} \ni b} q_{\mathcal{B}}$ and $1 - p_b = \sum_{\mathcal{B} \not\ni b} q_{\mathcal{B}}$, we have:

$$\bar{m} \leq \inf_{t \geq 0} \sum_{b=1}^q \left(p_b (k_b + t^2 w_b^2) + \frac{(1-p_b)}{2^{\frac{k_b}{2}-1} \Gamma(\frac{k_b}{2})} \phi_B(tw_b, k_b) \right) \quad (16)$$

Moreover, by the inequality I and (4), one may write

$$\begin{aligned} \bar{m} &\leq \inf_{t \geq 0} \sum_{b=1}^q k_b p_b + \\ &\sum_{i=1}^L \left[t^2 \omega_i^2 \left(\sum_{\mathcal{B} \supset \mathcal{P}_i} q_{\mathcal{B}} \right) + \frac{(\sum_{\mathcal{B} \not\supset \mathcal{P}_i} q_{\mathcal{B}})}{2^{\frac{k}{2}-1} \Gamma(\frac{k}{2})} \phi_B(t\omega_i, k) \right] = \sum_{b=1}^q k_b p_b + \\ &\sum_{i=1}^L \left(t^2 \omega_i^2 \alpha_i + \frac{(1-\alpha_i)}{2^{\frac{k}{2}-1} \Gamma(\frac{k}{2})} \phi_B(t\omega_i, k) \right), \end{aligned} \quad (17)$$

where we used $\alpha_i = \mathbb{P}(\mathcal{P}_i \subset \text{bsupp}(\mathbf{x})) = \sum_{\mathcal{B} \supset \mathcal{P}_i} q_{\mathcal{B}}$ and $1 - \alpha_i = \mathbb{P}(\mathcal{P}_i \not\subset \text{bsupp}(\mathbf{x})) = (\sum_{\mathcal{B} \not\supset \mathcal{P}_i} q_{\mathcal{B}})$. Since scaling is effectless on $P_{1,2,\omega^*}^\eta$, by minimizing the expressions in parentheses in (16) and (17) with respect to w_b and ω_i , one can get to the expressions (12) and (13). \blacksquare

REFERENCES

- [1] E. J. Candes and T. Tao, "Decoding by linear programming," *IEEE transactions on information theory*, vol. 51, no. 12, pp. 4203–4215, 2005.
- [2] D. L. Donoho, "For most large underdetermined systems of linear equations the minimal ℓ_1 -norm solution is also the sparsest solution," *Communications on pure and applied mathematics*, vol. 59, no. 6, pp. 797–829, 2006.
- [3] F. Parvaresh, H. Vikalo, S. Misra, and B. Hassibi, "Recovering sparse signals using sparse measurement matrices in compressed dna microarrays," *IEEE Journal of Selected Topics in Signal Processing*, vol. 2, no. 3, pp. 275–285, 2008.
- [4] M. Stojnic, F. Parvaresh, and B. Hassibi, "On the reconstruction of block-sparse signals with an optimal number of measurements," *arXiv preprint arXiv:0804.0041*, 2008.
- [5] T. Euler and T. Baden, "Computational neuroscience: Species-specific motion detectors," *Nature*, 2016.
- [6] M. Mishali and Y. C. Eldar, "Reduce and boost: Recovering arbitrary sets of jointly sparse vectors," *IEEE Transactions on Signal Processing*, vol. 56, no. 10, pp. 4692–4702, 2008.
- [7] Y. C. Eldar and M. Mishali, "Robust recovery of signals from a structured union of subspaces," *IEEE Transactions on Information Theory*, vol. 55, no. 11, pp. 5302–5316, 2009.
- [8] Y. M. Lu and M. N. Do, "A theory for sampling signals from a union of subspaces," *IEEE transactions on signal processing*, vol. 56, no. 6, pp. 2334–2345, 2008.
- [9] M. Mishali and Y. C. Eldar, "Blind multiband signal reconstruction: Compressed sensing for analog signals," *IEEE Transactions on Signal Processing*, vol. 57, no. 3, pp. 993–1009, 2009.
- [10] M. Mishali and Y. C. Eldar, "From theory to practice: Sub-nyquist sampling of sparse wideband analog signals," *IEEE Journal of Selected Topics in Signal Processing*, vol. 4, no. 2, pp. 375–391, 2010.
- [11] D. Amelunxen, M. Lotz, M. B. McCoy, and J. A. Tropp, "Living on the edge: Phase transitions in convex programs with random data," *Information and Inference: A Journal of the IMA*, vol. 3, no. 3, pp. 224–294, 2014.
- [12] D. Needell, R. Saab, and T. Woolf, "Weighted-minimization for sparse recovery under arbitrary prior information," *Information and Inference: A Journal of the IMA*, vol. 6, no. 3, pp. 284–309, 2017.
- [13] M. A. Khajehnejad, W. Xu, A. S. Avestimehr, and B. Hassibi, "Analyzing weighted ℓ_1 minimization for sparse recovery with nonuniform sparse models," *IEEE Transactions on Signal Processing*, vol. 59, no. 5, pp. 1985–2001, 2011.
- [14] N. Vaswani and W. Lu, "Modified-cs: Modifying compressive sensing for problems with partially known support," *IEEE Transactions on Signal Processing*, vol. 58, no. 9, pp. 4595–4607, 2010.
- [15] R. G. Baraniuk, V. Cevher, M. F. Duarte, and C. Hegde, "Model-based compressive sensing," *IEEE Transactions on Information Theory*, vol. 56, no. 4, pp. 1982–2001, 2010.
- [16] S. Oymak, M. A. Khajehnejad, and B. Hassibi, "Recovery threshold for optimal weight ℓ_1 minimization," in *Information Theory Proceedings (ISIT), 2012 IEEE International Symposium on*, pp. 2032–2036, IEEE, 2012.
- [17] S. Daei, F. Haddadi, and A. Amini, "Exploiting prior information in block sparse signals," *arXiv preprint arXiv:1804.08444*, 2018.
- [18] W. Xu, *Compressive sensing for sparse approximations: constructions, algorithms, and analysis*. PhD thesis, California Institute of Technology, 2010.
- [19] S. Misra and P. A. Parrilo, "Weighted ℓ_1 -minimization for generalized non-uniform sparse model," *IEEE Transactions on Information Theory*, vol. 61, no. 8, pp. 4424–4439, 2015.
- [20] M. Díaz, M. Junca, F. Rincón, and M. Velasco, "Compressed sensing of data with a known distribution," *Applied and Computational Harmonic Analysis*, 2017.
- [21] Z. Yang and L. Xie, "Exact joint sparse frequency recovery via optimization methods," *IEEE Transactions on Signal Processing*, vol. 64, no. 19, pp. 5145–5157, 2016.
- [22] M. M. Hyder and K. Mahata, "Direction-of-arrival estimation using a mixed ℓ_0 norm approximation," *IEEE Transactions on Signal Processing*, vol. 58, no. 9, pp. 4646–4655, 2010.
- [23] K. V. Mishra, M. Cho, A. Kruger, and W. Xu, "Spectral super-resolution with prior knowledge," *IEEE transactions on signal processing*, vol. 63, no. 20, pp. 5342–5357, 2015.
- [24] S. R. Becker, E. J. Candès, and M. C. Grant, "Templates for convex cone problems with applications to sparse signal recovery," *Mathematical programming computation*, vol. 3, no. 3, p. 165, 2011.